Chemical Science

Accepted Manuscript

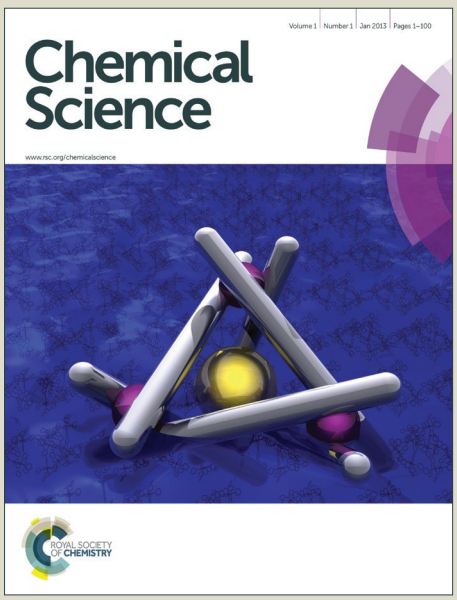

ROYAL SOCIETY OF CHEMISTRY

www.rsc.org/chemicalscience

Journal Name

COMMUNICATION

Energy Harvesting From Enzymatic Biowaste Reaction through Polyelectrolyte Functionalized 2D Nanofluidic Channels

Received 00th January 20xx,
Accepted 00th January 20xx

DOI: 10.1039/x0xx00000x

www.rsc.org/

Lei Lin, Ling Zhang, Lida Wang, and Jinghong Li*

Effective recycling biowaste energy in a compact system remains a great challenge. Here, we report a graphene-based energy harvesting system powered by enzymatic biowaste reaction through two-dimensional (2D) nanofluidic channels. The integrated 2D nanofluidic generator owns distinct advantages such as flexibility, low cost, and high output in ionic currents.

There is widespread concern that how to power the global economy in an efficient and clean way[1]. A way of addressing the sensitive issue may lie in the development of biowaste as an alternative energy resource. The exploration of those biowaste materials as a renewable energy resource in a compact and integrated system still remains a great challenge. In recent years, two-dimensional (2D) layered materials are considered as innovative candidates for the construction of energy conversion systems[2]. Owing to their 2D layered structure, superior mechanical and electrochemical performance[3], they exhibit surface-charge-governed ion transportation as the basis for power generation. Functionalized graphene sheets have high flexibility and can be horizontally extended to tens of micrometers[4]. These unique properties make the restacked graphene paper promising in construction of nanofluidic channels and nanoporous materials for membrane-based technologies, such as microbial fuel cell (MFC) and reverse dialysis (RED)[5]. Compared to conventional porous materials consisting of 1D or 3D fluidic channels, functionalized 2D layered materials provide much more straightforward ways to regulate the inner configuration of the fluidic channels and, therefore, the ion transportation property[6]. Guo et al. reported a nanofluidic energy conversion system based on the electrokinetic ion transport through a layered chemical converted graphene (CCG) membrane[7]. They convert mechanical energy in the water flow into electricity with the membrane-based device. But to date, the recycle of biowaste energy through 2D nanofluidic systems remains unexploited.

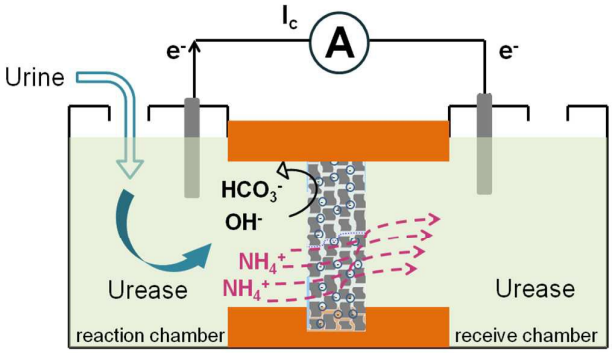

Scheme 1. Schematic representation of the biowaste-powered graphene nanofluidic generator. Negatively charged graphene-PAA composite membranes (GPM) preferentially permeate cations while exclude anions. When the urea molecules are catalyzed by urease, they release anions (OH^-, HCO_3^-) and cations (NH_4^+). The yielding NH_4^+ goes across the membrane under the chemical gradients from the reaction chamber to the receive chamber, resulting in net ionic current (I_c) and charge imbalance across the membrane (measured as an transmembrane electrical potential difference, E_m).

Here we demonstrate a graphene-based nanofluidic energy harvesting system powered by enzymatic biowaste reaction (Scheme 1). Polyacrylic acid (PAA) functionalized graphene composite membrane consisting of numerous interconnected 2D nanochannels between graphene layers forms a negatively charged 2D nanofluidic network within the membrane that endows the membrane material with cation-selectivity. Negatively charged graphene-PAA composite membranes (GPM) preferentially permeate cations while exclude anions. When the urea molecules are catalyzed by urease, they release anions (OH^-, HCO_3^-) and cations (NH_4^+). The yielding NH_4^+ goes across the membrane under the force of chemical gradients

L. Lin, L. Zhang, L. D. Wang, Prof. Dr. J. H. Li
Department of Chemistry, Beijing Key Laboratory for Analytical Methods and Instrumentation
Tsinghua University
Beijing 100084, China
E-mail: jhli@mail.tsinghua.edu.cn

Electronic Supplementary Information (ESI) available: [Experimental section, electrical measurement setup and composite membrane characteristics]. See DOI: 10.1039/x0xx00000x

from the reaction chamber to the receive chamber, resulting in net ionic current (I_c) and charge imbalance across the membrane (measured as an transmembrane electrical potential difference, E_m). When the ionic flow goes through the membrane in vertical direction driven by the enzymatic biowaste reaction, energy conversion is discovered as the generation of net transmembrane ionic current. The design strategy of the graphene-based 2D nanofluidic system can be generally extended to other 2D and polyelectrolyte materials for smart nanofluidic electrogenic devices and clean energy.

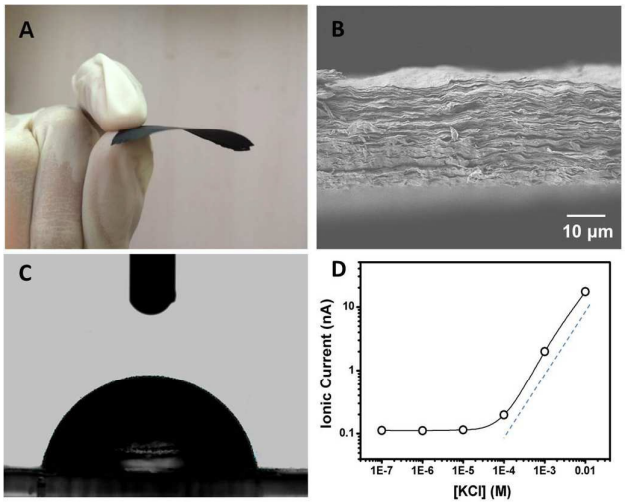

Figure 1. (A) A photograph of the self-supporting and flexible GPM after peeled off from the filtration film. (B) SEM image of the cross-section of a freeze-dried GPM showing layered microstrcture. (C) Contact angle (CA) measurement of the GPM, and the static CA was about 82.4°. (D) Concentration-dependent ionic conductance showing surface-governed ion transport below 10 mM.

Polyacrylic acid functionalized graphene composite membrane (GPM) was prepared by vacuum filtration of dispersed graphene-PAA complex colloid solution through a Poly(vinylidene fluoride) (PVDF) filter film[8] (Supporting information). The dispersions of GO and PAA were reduced by hydrazine and then filtered through a PVDF filter membrane by vacuum filtration. The as-prepared graphene-PAA composite membrane was peeled off from the filtration film. As can be seen from Figure 1A, the yielding GPMs are self-supporting. The thickness of the GPM can be readily tuned between 15 and 50 μm by applying desirable amount of graphene-PAA dispersion for filtration. SEM image in Figure S1B shows the surface topography of GPM. It can be found that the graphene film exhibits uniform morphology over large areas with wrinkles on the surface[9]. The cross-sectional view (Figure 1B) exhibits uniform layered structure of the freeze-dried GPM. The thickness of the membrane is about 25 μm from the cross-sectional view of SEM in Figure 1B. Since the XRD pattern of the GPM does not show a prominent peak, the interlayer spacing of the GHM can not be calculated from the characteristic XRD pattern. Additionally, the GPM is macroscopically hydrophobic (CA = 82.4°) and is not dissolved in water (Figure 1C). Electrostatic repulsion and steric hindrance from negative-charged polymers act as effective spacer to counter-balance the interlayer van der Waals interaction, which prevents the restacking of graphene sheets. We use attenuated total reflection flourier transformed infrared (ATR-FTIR) spectra to test the surface modification of graphene sheets. It is observed from Figure S2 that both PAA and graphene-PAA (G-PAA) show two characteristic peaks at 2928 cm^{-1} and 2867 cm^{-1}, assigning the C-H and C-C stretching frequency of PAA, respectively. While, as a comparasion, GO shows very weak absorption bands at the same place. The obvious signal difference indicates the successful functionalization of PAA onto the surface of graphene. Additionally, it is known that chemically reduced graphene obtained through hydrazine method precipitate as agglomerates owing to their hydrophobic nature. Our study shows that with the assistance of negatively charged polymer, graphene-PAA mixture is well-dispersed even after chemical reduction (Figure S1A in Supporting Information). The ATR-FTIR characteristics indicate the successful functionalization of PAA onto the surface of graphene, which is also consistent with previous reports[10].

In order to investigate the ion transport properties through the GPM, the composite film was mounted between two chambers of the testing cell filled with electrolyte solution. The transmembrane ionic conductance gradually decreases with the electrolyte concentration from 0.01 to 10^{-4} M, and then reaches equilibrium below 10^{-4} M (Figure 1D), suggesting a surface-charge-governed ionic transport behavior in lower salt concentration[11].

Figure 2 shows the typical response of the energy conversion under enzymatic biowaste reaction. Ag/AgCl electrodes were placed in individual buffer solution (0.01 mM KCl, 0.5 mg/mL urease, pH 7), which was connected with the test chamber through Agar-saturated KCl salt bridge (Scheme S1). This setup ensures the stability of the Ag/AgCl electrode, so that the measured ionic current (I_c) is solely generated from the enzyme-triggered ion transport through the graphene nanochannels. The transmembrane potential (E_m) and the diffusion current (Ic) were recorded with time elapsed (Figure 2). Without enzymatic catalysis, E_m and I_c tend to be constant. After the addition of urea, the catalytic reaction results in a significant rise in both I_c and E_m. This phenomenon may be attributed to two main reasons. Firstly, the assembled and rich-wrinkled structure of graphene forms numerous 2D nanochannels between neighbouring graphene sheets. All these nanochannels interconnect with each other and finally construct a 2D nanofluidic network within the membrane. Secondly, the modification with PAA introduces a large number of -COOH groups onto graphene surface. Under neutral condition, negatively charged PAA polymer effectively regulates the surface-charge-governed ion transportation of the 2D nanochannels. When the urea molecules are catalyzed by urease, numerous anions OH^-, HCO_3^- and cations NH_4^+ are released instantaneously. Forced by the concentration gradients, the yielding NH_4^+ transports across the membrane from the reaction chamber to the receive chamber, resulting in net ionic currents (I_c) and charge imbalance on both sides of the film (E_m). Peak values of 851 nA and 9.72 mV can be

reached within 8 min, suggesting the complete degradation of urea. The electric power density reaches 2.7 mW/m^2. Based on our experimental data and previous report[12], the maximum voltage (absolute value) and energy conversion efficiency (η_e) were calculated to be 177 mV and 0.3%, respectively (Scheme S2). These results indicate that the as-proposed graphene nanofluidic generators convert the energy of enzymatic biowaste reaction into electricity.

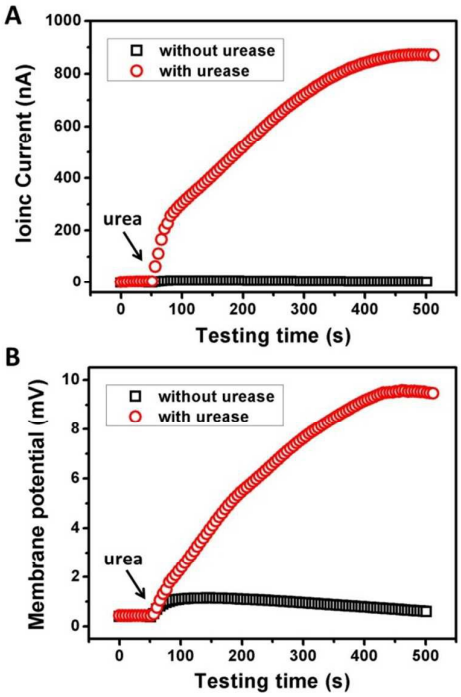

Figure 2. Response of the (A) ionic current and (B) membrane potential of GPM under the urea triggered enzymatic catalysis. Electrolyte: 0.01 mM KCl, pH 7. The concentrations of urease and urea were 0.5 mg/mL and 10 mM, respectively.

From the above discussion, we can see that the electrical response correlates with two main factors: the pH and concentration of the electrolyte solution. Figure 3A demonstrates the current and membrane potential characteristics of GPM in 0.01 mM KCl solution buffered from pH 5 to 9. It is observed that the maximum signal appears at pH 7. As mentioned above, the inner surface of GPM is full of carboxyl groups. Thus it is highly negatively charged under the neutral condition because the pK_a of PAA is estimated to be 4.7[13]. In other words, the carboxyl groups assembled on the graphene surface endow the 2D nanochannel with remarkable cation-selectivity[14]. Considering the dependence of negative charge density on pH, the 2D nanochannel permeates NH_4^+ much more rapidly under higher pH conditions[15], leading to higher ion current. On the contrary, excessively high pH cannot produce larger current and membrane potential generation. The reason is that the optimum pH of urease is 7.4 and its activity gradually declines along with the increasing pH.

As another crucial parameter, the influence of electrolyte concentration was also investigated. The enzymatic catalysis gradually increases with the decreasing KCl concentrations varied from 10 to 0.01 mM (Figure 3B). It may probably arise from the fact that higher ion concentration will generate strong shielding effect on the surface charge of 2D nanochannels, further leading to the weakening of ion-selective transport[16]. While, as a comparison, too low ionic concentration is also not benefit for the power generation. This is due to the increasing resistance in low-concentration electrolyte. Thus, the optimum electrolyte pH and concentration were chosen to be 7.0 and 0.01 mM, respectively.

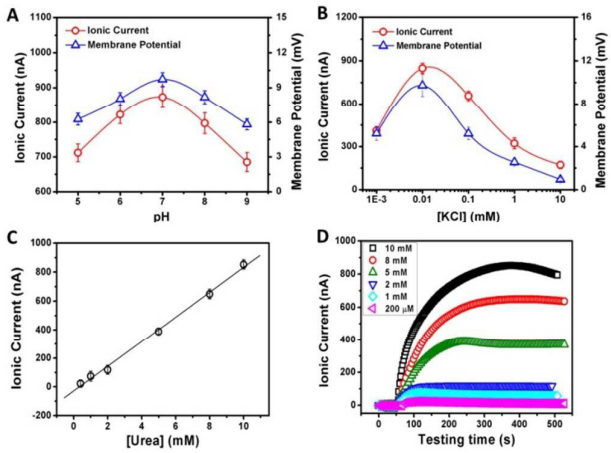

Figure 3. pH- (A) and concentration-dependence (B) of the ionic current and membrane potential generated from the urea-driven nanofluidic system. The concentrations of urease and urea were 0.5 mg/mL and 10 mM, respectively. (C) The dependence of ionic current on urea concentration. (D) Time elapse of ionic currents with respect to the urea concentration above 10 mM (The concentration of urease was 0.5 mg/mL).

The time elapses of ionic current with respect to the urea concentration are shown in Figure 3C. The concentrations of urease are identical in these measurements (0.5 mg/mL). After adding urea, ionic current gradually reaches the maximum value within 8 min. The amplitude of the resulting ionic current increases with the urea concentration from 0.2 mM to 10 mM at a constant rate of 82 nA/mM (Figure 3C). However, for high-concentration urea above 10 mM, negative impact to the generated ionic current is observed (Figure 3D). More urea could not generate larger ionic current. It may be originated from the reason that concentrated ammonium ions would simultaneously aggravate the interaction between ammonium ions and carboxylate ions, which could further result in negative impacts on cation diffusion and power generation.

To examine the possibility of the GPM for practical biowaste conversion, urine from human metabolism was added into the reaction chamber. Figure 4A and Figure 4B demonstrate that with the assistance of catalytic reaction, urine can also trigger significant power generation as the harvesting of both ionic current and membrane potential. The values of current, potential and electric power density are 600 nA, 7 mV and 1.3 mW/m^2, respectively. The above results justify its practical application for energy conversion using human biowaste. At the present stage, the output voltage is generally less than 10

mV. There is still a long way to go from being available for most of the real applications. From our point of view, there are two possible strategies to improve the performance of the 2D membrane. First, as key influencing factors, channel structure and charge density inside the 2D nanochannel could be further tuned through the optimization of film preparation steps. Second, enzymatic catalytic reaction could also be optimized to increase the charge selectivity of the membrane. Further efforts are needed toward a better performance of energy conversion through 2D nanofluidic networks.

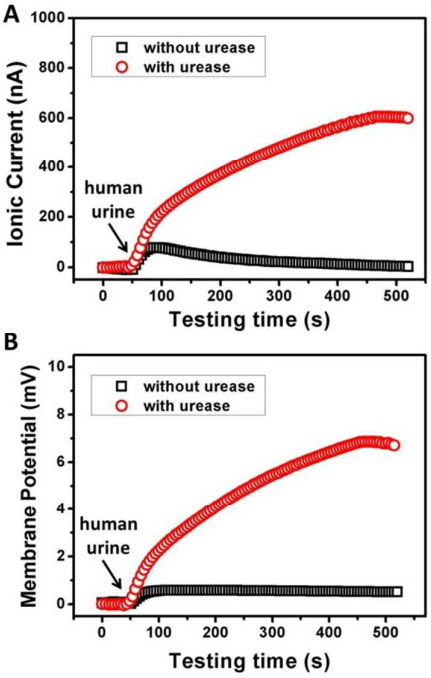

Figure 4. Response of the ionic current (A) and membrane potential (B) of the GPM using human urine triggered enzymatic catalysis. Electrolyte: 0.01 mM KCl, pH 7. The concentration of urease was 0.5 mg/mL.

In conclusion, we demonstrate an energy harvesting device powered by enzymatic biowaste reaction through polyelectrolyte functionalized 2D graphene nanofluidic channels. PAA-functionalized graphene forms layered structure, and constructing interconnected 2D nanofluidic networks inside the membrane. Negatively charged GPM owns the surface-charge-governed ion transport, preferentially permeating counter-ions while excluding co-ions. Under the force of enzymatic biowaste reaction, energy conversion is discovered as the generation of ionic current and electric potential across the membrane. Our results suggest that the as-proposed 2D graphene-PAA nanosystem shows sensitively and promptly response to human urine. We believe that the strategy is generally applicable to other type of nanofluidic devices for energy harvesting.

Acknowledgements

This work was financially supported by the National Natural Science Foundation of China (No. 21235004, No. 21327806).

References

1 J. P. H. van Wyk, *Trends Biotechnol.* 2001, **19**, 172.
2 C. N. Yeh, K. Raidongia, J. Shao, Q. H. Yang, J. Huang, *Nat. Chem.* 2015, **7**, 166; X. Huang, X. Qi, F. Boey, H. Zhang, *Chem. Soc. Rev.* 2012, **41**, 666; D. Li, R. B. Kaner, *Science* 2008, **320**, 1170; D. Li, M. B. Mueller, S. Gilje, R. B. Kaner, G. G. Wallace, *Nat. Nanotechnol.* 2008, **3**, 101; W. Guo, L. Jiang, *Sci. China Mater.* 2014, **57**, 2.
3 C. Cheng, D. Li, *Adv. Mater.* 2013, **25**, 13; Q. Cheng, M. Wu, M. Li, L. Jiang, Z. Tang, *Angew. Chem. Int. Ed.* 2013, **52**, 3750; X. Huang, Z. Yin, S. Wu, X. Qi, Q. He, Q. Zhang, Q. Yan, F. Boey, H. Zhang, *Small* 2011, **7**, 1876; X. Yang, L. Qiu, C. Cheng, Y. Wu, Z. F. Ma, D. Li, *Angew. Chem. Int. Ed.* 2011, **50**, 7325.
4 K. Raidongia, J. X. Huang, *J. Am. Chem. Soc.* 2012, **134**, 16528.
5 R. D. Cusick, Y. Kim, B. E. Logan, *Science* 2012, **335**, 1474; H. Wang, H. Feng, J. Li, *Small*, 2014, **10**, 2165; S. Ci, P. Cai, Z. Wen, J. Li*, *Sci. China Mater.*, 2015, **58**, 496.
6 W. Guo, T. Ye, L. Jiang, *Acc. Chem. Res.* 2013, **46**, 2834.
7 W. Guo, C. Cheng, Y. Wu, Y. Jiang, J. Gao, D. Li, L. Jiang, *Adv. Mater.* 2013, **25**, 6064.
8 J. Y. Lee, I. In, *Chem. Lett.* 2012, **41**, 127.
9 H. Feng, R. Cheng, X. Zhao, X. Duan, J. Li, *Nat. Commun.* 2013, **4**, 1539; L. Tang, H. Feng, J. Cheng, J. Li, *Chem. Commun.* 2010, **46**, 5882; L. Wu, H. Feng, M. Liu, K. Zhang, J. Li, *Nanoscale* 2013, **5**, 10839.
10 J. Q. Liu, L. Tao, W. R. Yang, D. Li, C. Boyer, R. Wuhrer, F. Braet, T. P. Davis, *Langmuir* 2010, **26**, 10068; J. Y. Hong, K. Y. Shin, O. S. Kwon, H. Kang, J. Jang, *Chem. Commun.* 2011, **47**, 7182; J. Y. Lee, I. In, *Chem. Lett.*, 2012, **41**, 127.
11 R. B. Schoch, J. Han, P. Renaud, *Rev. Mod. Phys.* 2008, **80**, 839.
12 L. P. Wen, Y. Tian, Y. L. Guo, J. Ma, W. D. Liu, L. Jiang, *Adv. Funct. Mater.* 2013, **23**, 2887.
13 X. Hou, F. Yang, L. Li, Y. L. Song, L. Jiang, D. B. Zhu, *J. Am. Chem. Soc.* 2010, **132**, 11736.
14 J. Cervera, B. Schiedt, R. Neumann, S. Mafe, P. Ramirez, *J. Chem. Phys.* 2006, **124**, 104706; J. Cervera, B. Schiedt, P. Ramirez, *Europhys. Lett.* 2005, **71**, 35; Z. Siwy, A. Fulinski, *Phys. Rev. Lett.* 2002, **89**, 198103.
15 X. Hou, Y. Liu, H. Dong, F. Yang, L. Li, L. Jiang, *Adv. Mater.* 2010, **22**, 2440.
16 K. Y. Chun, P. Stroeve, *Langmuir* 2002, **18**, 4653; R. Karnik, K. Castelino, R. Fan, P. Yang, A. Majumdar, *Nano Lett.* 2005, **5**, 1638; D. Stein, M. Kruithof, C. Dekker, *Phys. Rev. Lett.* 2004, **93**, 035901; F. H. J. van der Heyden, D. J. Bonthuis, D. Stein, C. Meyer, C. Dekker, *Nano Lett.* 2007, **7**, 1022.